

Density Effects on Soil-Water Characteristics, Soil-Gas Diffusivity, and Emissions of N₂O and N₂ from a Re-packed Pasture Soil

Chamindu Deepagoda T. K. K.

Dep. of Civil Engineering
Faculty of Engineering
Univ. of Peradeniya
20400 Peradeniya, Sri Lanka

and

Dep. of Soils and Physical Sciences
PO Box 85084
Lincoln Univ.
Lincoln 7647, Canterbury, NZ

T. J. Clough*

Dep. of Soils and Physical Sciences
PO Box 85084
Lincoln Univ.
Lincoln 7647, Canterbury, NZ

S. M. Thomas

New Zealand Inst. for Plant & Food
Research Limited
Private Bag 4704, Christchurch, NZ

N. Balaine

Dep. of Soils and Physical Sciences
PO Box 85084
Lincoln Univ.
Lincoln 7647, Canterbury, NZ

B. Elberling

Dep. of Geosci. & Nat. Resour. Mgmt.
Center for Permafrost (CENPERM)
Univ. of Copenhagen
Øster Voldgade 10
DK-1350 Copenhagen, Denmark

Density-induced soil structural changes may potentially alter both soil total porosity and soil pore size distribution, and thus change the soil's water retention characteristics, gas diffusion and transport properties, and subsequent greenhouse emissions. In this study, we characterized and parameterized water retention, pore size distribution, gas diffusivity and cumulative emissions of nitrous oxide (N₂O) and nitrogen (N₂) fluxes in a differently compacted silt-loam sampled from a grazed pasture in Lincoln, New Zealand. The soils used for the simulations were subjected to five different density treatments (1.1, 1.2, 1.3, 1.4, 1.5 Mg m⁻³), subsequently saturated and successively drained to 11 matric potentials at which water retention, gas diffusivity and flux measurements were performed. Results show strong correlations between best-fit soil-water characteristic parameters and the density levels. A recent predictive gas diffusivity model developed for undisturbed soils was modified to better characterize the measured gas diffusivity data in sieved-repacked pasture soils. Further, two exponential and linear parametric models were developed to adequately parameterize the observed fingerprints of cumulative (35-d) N₂O and N₂ fluxes, respectively. Results clearly distinguished the density-induced changes in pore structure, pore size distribution, gas diffusivity and emission of gas fluxes and hence provide useful implications for pasture management to reduce future emission of greenhouse gases. Results particularly highlighted the importance of ensuring a diffusivity ≥ 0.038 to limit extensive emission of N₂O and N₂ fluxes. The improved parametric models and parameter correlations provide valuable numerical insight to better characterize density-dependent behavior in soil physical properties and functions.

Abbreviations: SWC, soil-water characteristic.

Grazed pastures constitute an essential component in agricultural systems from which substantial amounts of nitrous oxide (N₂O) are released to the atmosphere (Oenema et al., 2005). The N₂O molecule is a potent greenhouse gas with a global warming potential 298-fold greater than CO₂ over a 100-yr span (IPCC, 2014). Emissions of N₂O from pasture soils are mainly associated with the deposition of ruminant urine (Selbie et al., 2015). Microbial mechanisms responsible for the production of N₂O in soil include, but are not limited to, nitrification, nitrifier-denitrification and denitrification (Wrage et al., 2001, 2018). Anaerobic soil environments not only promote N₂O formation, since N₂O is an obligate intermediary in denitrification, but they also favor the complete denitrification of N₂O to N₂ (Firestone, 1982). While losses of N₂ are environmentally benign they represent an economic loss of N inputs. When oxygen becomes limiting in the soil nitrifiers may opt to denitrify nitrite (NO₂⁻) to N₂O, rather than oxidize it to nitrate (NO₃⁻), in an effort to conserve oxygen and energy (Wrage et al., 2018). Under aerobic conditions N₂O is released, during nitrification, as a by-product of NH₃ oxidation to NO₂⁻. Thus, the dominant N₂O

Core Ideas

- A predictive gas diffusivity model for undisturbed soils was modified for sieved-repacked pasture soils.
- Density-induced changes in soil physical attributes along with gaseous fluxes help identify N₂O mitigation.
- Maintaining well-aerated conditions and a soil-gas diffusivity of >0.038 may be a mechanism for keeping N₂O and N₂ fluxes low.

Soil Sci. Soc. Am. J. 83:118–125

doi:10.2136/sssaj2018.01.0048

Received 23 Jan. 2018.

Accepted 2 Nov. 2018.

*Corresponding author (Timothy.Clough@lincoln.ac.nz).

© Soil Science Society of America. This is an open access article distributed under the CC BY license (<https://creativecommons.org/licenses/by/4.0/>).

production pathway depends not only on the substrate supply but also on the soil's moisture status and level of aeration. It is likely that N₂O emissions under a given ambient condition are triggered by a combination of the above mechanisms causing an overprint of N₂O, which is difficult to be traced back to the exact source mechanism(s).

Since the density of soil can potentially control a soil's moisture status and its level of aeration, soil density becomes an important soil physical parameter controlling both N₂O and N₂ emissions from grazed pasture systems (Ball, 2013). An improved understanding of gas emissions from soil is likely to occur through the use of pore-scale models due to the influence of pore continuity and size on soil gas production, transport and release (Ball, 2013). Density essentially alters the soil physical integrity by relocating soil-solid constituents and changing the porosity and size distribution of pores. As a result, transport and retention characteristics of soil-water and soil-gas, which mutually share the pore space and which are also pore size-dependent, become density-controlled. Past studies have revealed marked effects of soil density on soil-water retention, gas diffusivity (Croney and Coleman, 1954; Gupta et al., 1989) and hydraulic conductivity (Gent et al., 1983). Implications of enhanced soil density in grazed pastures, due to animal treading and excessive use of agricultural machinery, are detailed in the literature. Studies provide evidence for reduced pasture yields due to animal trampling in grazed pasture, which were found to be more severe under wet conditions and high stocking rates (Cannell 1977; Carter 1988; Drewry, 2006). Negative impacts of soil compaction, due to mechanized implements, on pasture productivity have also been reported, but their effects are not as widespread within paddocks compared with animal trampling due to their reduced spatial distribution (Drewry, 2006; Sigua and Coleman, 2009).

Mixed responses of microbial activity to soil compaction, on the other hand, have been reported in the literature (Dick et al., 1988; Ponder and Tadros, 2002; Breland and Hansen, 1996). Recent studies directly linking density effects on N₂O emissions are also available in the literature (e.g., Balaine et al., 2013, 2016).

The soil-gas diffusion coefficient (D_p , m² s⁻¹) is the single most important parameter describing gas diffusion in soil (Buckingham, 1904). Scaling D_p with the diffusion coefficient of the same gas in free air (D_o , m² s⁻¹) at the same temperature and pressure yields soil-gas diffusivity, D_p/D_o . Since scaling generally normalizes the controlling effects which are common in D_p and D_o (e.g., characteristics of the gas molecules, temperature, pressure), D_p/D_o becomes a function only of the properties of the soil facilitating gas diffusion, mainly the air-filled porosity and the tortuosity of the functional gaseous phase. As the presence of water decreases the air-filled porosity and increases the tortuosity, soil moisture gives a two-fold effect on D_p/D_o , thereby making D_p/D_o strongly moisture dependent (Moldrup et al., 2000). The literature also demonstrates that the aeration conditions for plant growth are better represented by D_p/D_o rather than air-filled porosity (Gislerød, 1982; Allaire et al., 1996), and that D_p/D_o is an appropriate predictor of soil-gas fluxes (Balaine et al., 2016).

The main objective of this study was to parameterize the measured properties of soil-water retention, D_p/D_o , and both N₂O and N₂ fluxes under varying soil density using existing and suggested parametric functions, and to thereby investigate their integrated behavior linking to soil density. We considered data in the literature and measurements obtained from a controlled laboratory study which used soil sampled from a grazed pasture site. Soil bulk density, the controlled soil physical parameter, was used as the primary measure of the degree of densification and/or compaction when the density-induced effects on the measured properties were compared. The scope of the present study will be limited to a single soil texture with a discussion of potential implications to differently-textured soils.

MATHEMATICAL MODELING

Soil-Water Characteristic and Pore Size Distribution

We invoke here the van Genuchten (1980) model to parameterize the relationship of matric potential (ψ) to soil moisture content (θ), given its wide number of applications and relevance to ecological practices, to characterize soil-water retention as follows:

$$\theta(\psi) = \theta_r + (\theta_s - \theta_r) \left(\frac{1}{1 + |\alpha\psi|^n} \right)^m \quad [1]$$

where θ_s is the soil water content at saturation (cm³ cm⁻³), θ_r is the residual water content (cm³ cm⁻³), α is model scaling factor (cm⁻¹), and n and m are model shape factors. The shape factor m is usually constrained by linking it to n (e.g., $m = 1 - 1/n$), however, in this study we used m also as an unconstrained (fitting) parameter to obtain an additional degree of freedom.

The first derivative of the above soil-water characteristic (SWC) function (Eq. [1]) yields the pore size density function which can be written as (Durner, 1994):

$$\frac{d\theta(r)}{d \log_{10} r} = \frac{d\theta(\text{pF})}{d(\text{pF})} = \frac{d\theta(\psi)}{d \log_{10} |\psi|} = \frac{d\psi}{d \log_{10} |\psi|} = \frac{d\theta(\psi)}{d\psi} = [\log_e 10] |\psi| \frac{\partial \theta}{\partial \psi} \quad [2]$$

where r (cm) is the pore radius and $\text{pF} = \log |-\psi|$, 10⁻³ kPa | (Schofield, 1935). Note that when $\theta_r = 0$ (in Eq. [1]), the second term (right side) of Eq. [2] becomes

$$\psi \frac{\partial \theta}{\partial \psi} = \frac{\theta_s m n \alpha \psi}{[1 + (\alpha\psi)^n]^{1+m}} \quad [3]$$

Soil-Gas Diffusivity

Soil compaction effects in relation to soil-gas diffusivity (D_p/D_o) model development have been discussed since the pioneering work of Buckingham (1904), who concluded that *diffusivity is not greatly dependent on soil structure* but the [air-filled] porosity (ϵ , cm³ cm⁻³) of soil. Consequently, early-stage diffusivity models were simply functions of ϵ (e.g., Penman, 1940; Millington, 1959; Marshall, 1959). Later models, however, in-

cluded the total porosity (Φ , $\text{cm}^3 \text{cm}^{-3}$) in addition to air-filled porosity to account for the effects of water and water-induced tortuosity, which indirectly reflected the effect of density as well. Gas diffusivity models directly focused on the density effects are also available in the literature, for example the density-corrected gas diffusivity model (Chamindu Deepagoda et al., 2010), which takes the form of:

$$D_p/D_o = 0.1 \left[2 \left(\frac{\varepsilon}{\Phi} \right)^3 + 0.04 \left(\frac{\varepsilon}{\Phi} \right) \right] \quad [4]$$

in which the constant scale factors are best-fit values to the measured data. Note that Eq. [4] was essentially developed using undisturbed soils in which natural cementing and/or bonding effects caused by the organic matter and adsorbed water could potentially increase the gas-phase tortuosity. In sieved and repacked soils, however, de-structuring eliminates the natural bonding effects and hence also the additional gaseous-phase tortuosity, resulting in an increase in gas diffusivity at the same air-filled porosity. To account for this, we generalized Eq. [4] while retaining its original form as follows:

$$D_p/D_o = A \left[2 \left(\frac{\varepsilon}{\Phi} \right)^B + C \left(\frac{\varepsilon}{\Phi} \right) \right] \quad [5]$$

where A , B , and C are model parameters to be determined by fitting to the measured data. We emphasize that Eq. [5] is intended to be used as a *descriptive* parametric function which can readily represent the measured data and hence its relation to density, but not necessarily as a predictive model for sieved-repacked soils in general.

Cumulative N_2O -N and N_2 -N Fluxes

To express cumulative N_2O -N fluxes ($J_{\text{N}_2\text{O}}$), we propose an exponential decay function in the following form:

$$J_{\text{N}_2\text{O}} = J_{m,\text{N}_2\text{O}} + (J_{m,\text{N}_2\text{O}} - J_{0,\text{N}_2\text{O}}) \exp \left[\ln(0.05) \frac{D_p/D_o}{(D_p/D_o)^*} \right] \quad [6]$$

where $J_{0,\text{N}_2\text{O}}$ and $J_{m,\text{N}_2\text{O}}$ are cumulative N_2O -N fluxes when the gas diffusivity is zero and when the gas diffusivity is fully mobilized, respectively. The threshold diffusivity, $(D_p/D_o)^*$, denotes the gas diffusivity above which the cumulative flux shows only a 5% drop from the total decrease.

Similarly, to describe cumulative N_2 fluxes (J_{N_2}), we propose a two-step linear function as follows:

$$J_{\text{N}_2} = J_{m,\text{N}_2} + (J_{0,\text{N}_2} - P_{m,\text{N}_2}) \left[1 - \frac{D_p/D_o}{(D_p/D_o)^*} \right], \quad D_p/D_o \leq (D_p/D_o)^* \quad [7]$$

$$J_{\text{N}_2} = J_{m,\text{N}_2}, \quad D_p/D_o > (D_p/D_o)^* \quad [8]$$

where J_{0,N_2} and J_{m,N_2} are similar parameters as described above for N_2O but correspond to N_2 fluxes, and $(D_p/D_o)^*$ denotes the gas diffusivity at which the linear transition occurs.

MATERIALS AND METHODS

In this study, we considered measured data from the literature (Balaine et al., 2013, 2016) to parameterize the models and for further analyses. The soils considered were sampled at a depth of 0 to 15 cm on a pasture site at Duncan Block ($43^\circ 38' 0.7''$ S, $172^\circ 29' 40''$ N) managed by Lincoln University, New Zealand. The soil was characterized as a silt loam and was identified as a Templeton silt loam, Typic Immature Pallic under the New Zealand Soil Classification system (Hewitt, 1998). The air-dried and sieved (<2 mm) soil received density treatments: five levels of bulk density were 1.1, 1.2, 1.3, 1.4, and 1.5 Mg m^{-3} . The samples were compacted into stainless steel cylinders (7.3 cm i.d., 4.1 cm depth) according to treatment. To obtain a uniform soil bulk density, the soil cores were compressed uniaxially, 1-cm depth at a time, with the surface loosened between compaction of layers. Soil cores then received a ^{15}N labeled urea solution that replicated a bovine urine deposition event (700 kg N ha^{-1}), as described by Balaine et al. (2016), followed by drainage at 11 levels of matric potential (ψ): $-1.0, -1.5, -2.0, -3.0, -4.0, -5.0, -6.0, -7.0, -8.0, -9.0$, and -10 kPa . Soil-gas diffusivity (D_p/D_o) and N_2O and N_2 flux measurements were conducted at each matric potential over a 35-d period (Balaine et al., 2016).

The measurements of D_p/D_o were conducted using a one-chamber diffusion apparatus (Taylor, 1949). For the flux measurements, each sample was placed in a 1-L tin container (10.4 cm diameter by 12.0 cm height) which was then sealed with an air-tight lid equipped with a rubber septum. Gas samples for N_2O (10 mL) were taken at 0, 15, and 30 min intervals and analyzed with a gas chromatograph (SRI-8610, Torrance, CA) as previously described (Clough et al., 2006). The N_2O fluxes were calculated following Hutchinson and Mosier (1981). A single gas sample (15 mL) was also taken after 2 h for N_2 flux determination. A detailed account of gas sampling procedures, methodology, instruments used, and calculation methods are given by Balaine et al. (2016).

RESULTS AND DISCUSSION

The soil-water characteristic (SWC) is generally considered to be a good indicator of the degree of soil densification and/or compaction (Gupta et al., 1989) as evidenced by the measured SWC at different density levels (Fig. 1).

The decreasing saturated water content (θ_s) and increasing air-entry potential and/or bubbling pressure (P_b , kPa) with increasing density are clearly evident from the results and hence corroborate the observations of previous studies (e.g., Croney and Coleman, 1954). It is also clear that the water held at higher matric potential increases, while the water held at low matric potential decreases, with increasing compaction as also discussed in the literature (Gupta et al., 1989). The above observations are clear signs of the decreasing total porosity and associated shift in relative proportion of pore sizes on compaction, as reflected by the change in pore size distribution (discussed later). Noticeably, the density effects in SWC become less evident at low matric potentials (e.g., below -1000 kPa) since the water is

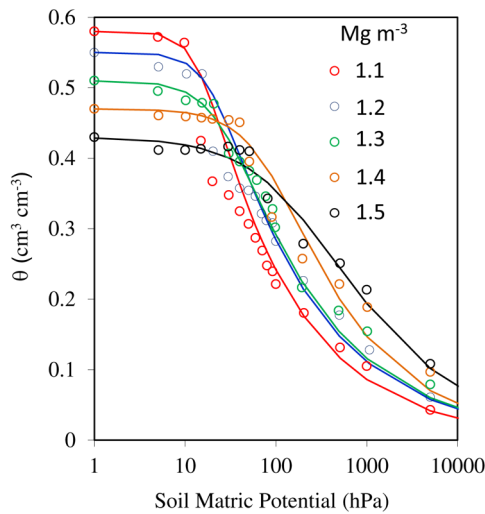


Fig. 1. Soil moisture content (θ , $\text{cm}^3 \text{cm}^{-3}$) as a function of soil matric potential (ψ) for the 2-mm sieved pasture soil repacked at five different densities (open circles) together with parameterized van Genuchten model, Eq. [1] (solid lines). Data are from Balaine et al. (2016).

held as thin water films around solid particles rather than occupying the pores thus making the volumetric water content (θ_v , $\text{m}^3 \text{water m}^{-3} \text{soil}^{-3}$) less descriptive of the density-induced SWC differences. In fact, a SWC based on the gravimetric water content (θ_g , $\text{g water g dry soil}^{-1}$) may better reflect the density effects at lower matric potentials (not shown). Importantly, the density induced differences in SWC are texture dependent; Hill and Sumner (1967) concluded that sandy soil holds more water with increasing bulk density at a given matric potential as opposed to sandy loam and clay loam. Clay soils, with a higher capacity for hygroscopic water (i.e., chemically adsorbed to internal structure of clay particles) may hold more water at lower matric potentials on compaction when compared to other textures. Figure 1 also shows (solid lines of corresponding colors) the best-fit parameterized van Genuchten model (Eq. [1]). Note that the soils at lower density (1.1 and 1.2 Mg m^{-3}) show a slightly aggregated behavior which diminishes with increasing density, however we

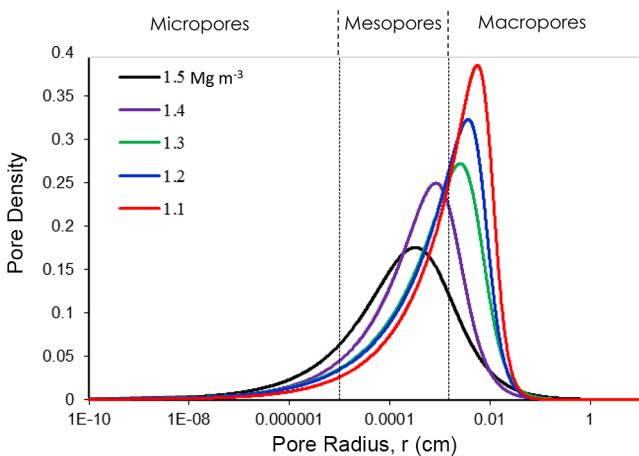


Fig. 2. The van Genuchten (1980) model-derived pore size distribution (Eq. [2] and [3]) for the soils at five density levels (denoted by different colors). Three different pore regimes: micropores ($<0.02 \mu\text{m}$), mesopores ($0.02\text{--}30 \mu\text{m}$) and macropores ($>30 \mu\text{m}$) are also shown.

disregarded this effect and regarded them numerically equally in modeling. Generally, we obtained a good description with the parameterized van Genuchten model, with model parameters well-correlated with the density as described below.

Figure 2 shows the shift in the van Genuchten model-derived pore size distribution (Eq. [2]) at increasing density across different pore regimes: micropores ($<0.02 \mu\text{m}$ pore dia.), mesopores ($0.02\text{--}30 \mu\text{m}$) and macropores ($>30 \mu\text{m}$). The distinct decrease in the peak height (pore density) implies a decrease in porosity, while the peak-shift is associated with the resultant change in pore size regime. Decreasing macroporosity and an increase in mesoporosity and microporosity with increasing compaction is a previously recognized phenomena (Yahya et al., 2011). This shift in dominant pore regime on compaction may potentially cause a significant effect on water and air phase configuration in soils. Decreases in large aerated pores, those that readily drain at low matric potentials, and an increase in capillary pores, those that remain water-filled at low matric potentials, produce a two-pronged impact on diffusion-controlled gas movement and results in a more favorable anaerobic environment for denitrification. Note also that the increased density of micropores results in higher air-entry pressures (P_b , kPa) as soils are compacted as shown by the SWC (Fig. 1a).

The best-fit van Genuchten parameters are shown in Fig. 3 as a function of bulk density. Interestingly, van Genuchten parameters α (kPa^{-1}) and n showed strong negative linear relations with density whereas m showed a strong positive and nonlinear (exponential) relation. Since P_b corresponds to $1/\alpha$, a power-law relation exists between the P_b and the soil density (i.e., $P_b \propto \rho^8$; $r^2 = 0.9$; not shown). The strong linear decrease in the maximum occurring pore diameter (i.e., the diameter corresponding to the peak of the pore size distribution in Fig. 2) with increasing density, implies a linear decrease in dominant pore size with compaction.

The measured soil-gas diffusivity (D_p/D_o) as a function of normalized air-filled porosity (ϵ/Φ) is shown (in different colors) in Fig. 4 for the five density levels, together with the proposed modified density-corrected model (solid line) (Eq. [5]) with best-fit values of A ($= 0.4$), B ($= 5.2$), and C ($= 0.04$). Shown also in Fig. 4 are the original density-corrected gas diffusivity model (dotted line) and the intact soil data (shown in gray color) used to derive the density-corrected model (data from Chamindu Deepagoda et al., 2010). Note that the selected intact soil data also showed a marked difference in naturally occurring density with bulk density ranging between 1.2 to 1.9 Mg m^{-3} (Chamindu Deepagoda et al., 2010). Importantly, although the density-induced effects are normalized when the D_p/D_o is compared against normalized air-filled porosity (ϵ/Φ) at individual soil structure states (i.e., intact and repacked), normalization does not necessarily occur across states. At high water saturation, D_p/D_o is predominantly moisture-controlled and the water-induced scatter in measurements (particularly in intact soils) makes it difficult to distinguish the intact and repacked soils. However, the differences in D_p/D_o are more evident when the soils become drier ($\epsilon/\Phi > 0.5$). In this study, however, we consider the best-fit

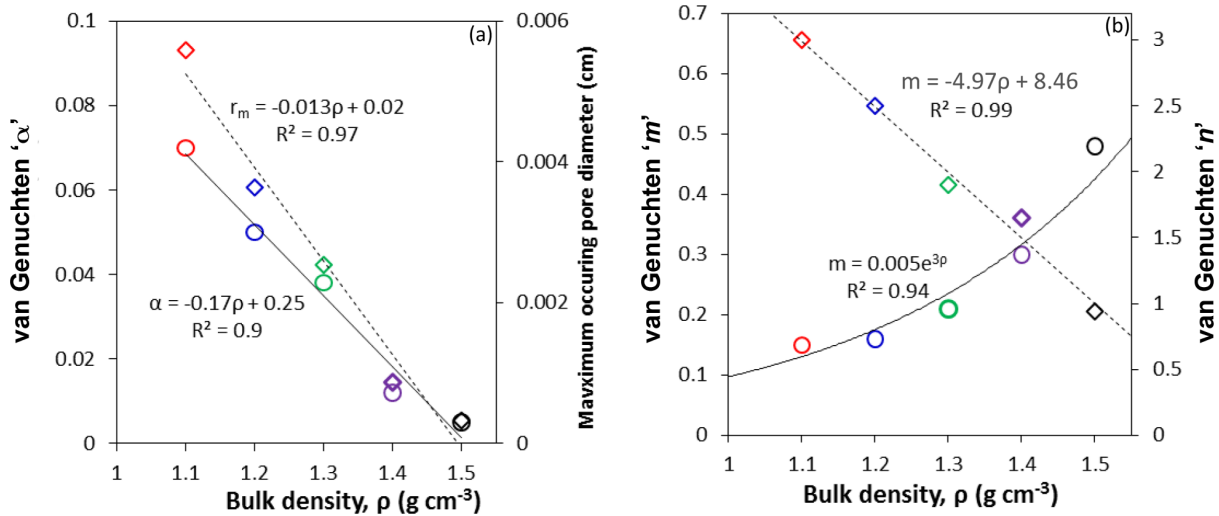


Fig. 3. Variation of van Genuchten model (Eq. [1]) parameters α (a, open circles), m (b, open circles), and n (b, open diamonds) against bulk density. The maximum occurring pore diameter as a function of density (a, open diamonds) is also shown. Solid lines denote the best-fit relations for above variations.

model (Eq. [5]) as a descriptive model which simply describes the measured D_p/D_o data, and await more measurements, across a wider range of density levels, to validate the model and check its predictive capability.

The 35-d cumulative $\text{N}_2\text{O-N}$ and $\text{N}_2\text{-N}$ fluxes as a function of D_p/D_o are shown in Fig. 5. The two proposed parametric functions, Eq. [6] for $\text{N}_2\text{O-N}$ and Eq. [7] and [8] for $\text{N}_2\text{-N}$, are also shown (solid lines) with optimized parameters. The threshold gas diffusivity for both gases, $(D_p/D_o)^*$ ($= 0.038$), is an important parameter which conceptually denotes a critical gas diffusivity above which the denitrification-derived gas emissions can be virtually sustained at a minimum level. Notably, measured cumulative $\text{N}_2\text{O-N}$ and diffusivity data from Owens et al. (2016) also imply a similar threshold gas diffusivity. In practice, it is therefore important to ensure that D_p/D_o is maintained above the $(D_p/D_o)^*$ to limit any exponential increase in the emissions of N_2O . Revisiting Fig. 4, the $(D_p/D_o)^*$ corresponds to a relative air-filled porosity (ϵ/Φ) of 0.52 irrespective of the density, which was not achieved at higher density (1.5 Mg m^{-3}) conditions. Potentially, the magnitude of $(D_p/D_o)^*$ may also vary depending on other factors such as soil physical and geochemical conditions favoring denitrification or oxygen consumption, for example, the soil type may affect these by influencing substrate supply and microbial community composition and function.

The results of the model parameterizations are summarized in Table 1.

Combining all the density-related parametric functions described above, flux emissions at the nexus of water retention and gas diffusivity can be examined. Figure 6 shows density, soil matric potential (in pF), and gas diffusivity relations in a 3-D Cartesian system. The color contours denote the corresponding soil-water contents. Soil gas diffusivity contours (0.01 to 0.28) are also shown (in black color). The threshold diffusivity with respect to cumulative N_2O flux emissions, $(D_p/D_o)^*$ (~ 0.04), is shown as a dark black contour for distinction. We broadly iden-

tify three regions with respect to pF: (i) pF of 0 to 1.75 in which the moisture content (held predominantly in large pores) is high but varies only a little across density. Due to the high moisture-controlled effects, gas diffusivity is very small (< 0.005) in this region, (ii) pF of 1.75 to 3.75 in which the interplay between soil-water and soil-gas is pronounced and both (water retention and diffusion) effects are highly density dependent. Interestingly, both moisture content and gas diffusivity contours tend to follow

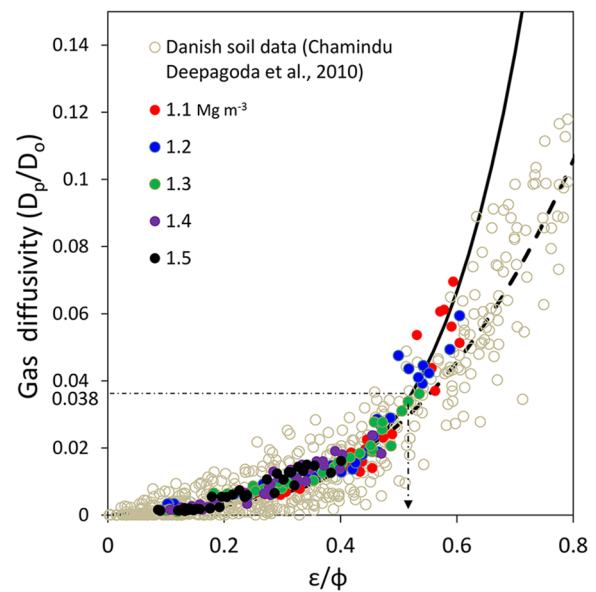


Fig. 4. Soil-gas diffusivity, D_p/D_o , as a function of relative air-filled porosity (ϵ/Φ) for the sieved pasture soils at five compaction levels (shown in differently colored circles). The modified density-corrected D_p/D_o model, Eq. [5], with model parameters ($A = 0.4$, $B = 5.2$, $C = 0.04$) best-fit to the measured data is shown (in solid line). Also shown are the original density-corrected D_p/D_o model (Eq. [5]) with $A = 0.1$ and $B = 3$ (in dotted line) and the intact soil data (gray circles) used to develop the density-corrected model. The threshold diffusivity for N_2O and N_2 fluxes, $(D_p/D_o)^*$ ($= 0.038$), is also shown for perspective. Data are from Balaine et al. (2016) and Chamindu Deepagoda et al. (2010).

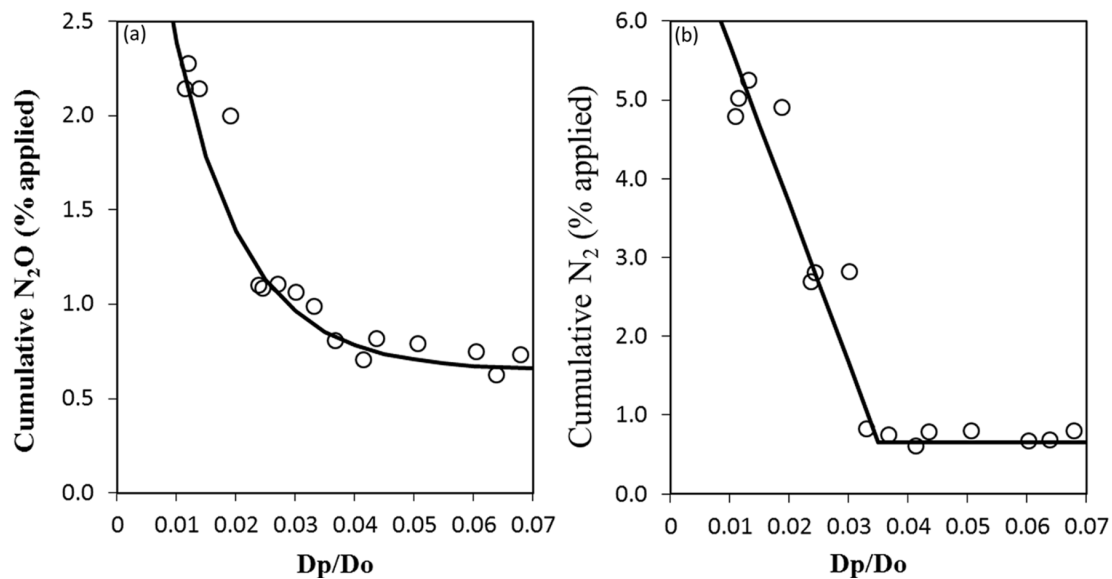


Fig. 5. Measured cumulative (35-d) fluxes (as percentage of N applied) for (a) N₂O-N and (b) N₂-N as a function of gas diffusivity D_p/D_o for a repacked pasture soil. The best-fit parametric functions are shown in solid lines. Data are from Balaine et al. (2016).

each other in this region irrespective of the density, due to their strong link via relative air-filled porosity (ϵ/Φ), and (iii) pF of >3.75 , in which the moisture content is small ($<0.05 \text{ cm}^3 \text{ cm}^{-3}$) and present as chemically absorbed or bound water to the solid particles and hence no significant density-dependent effects occur. Gas diffusivity in this region is mostly dependent on the amount of air-filled porosity (due to lack of water-induced effects). Overall, the figure shows a consistent complementary behavior of moisture retention and gas diffusivity across the observed range of matric potential and density.

Finally, the simulated characteristic diffusivity (D_p/D_o) functions are illustrated in Fig. 7 as related to density: (a) D_p/D_o vs. pF together with air-filled porosity contours (in black lines) and (b) D_p/D_o vs. air-filled porosity (ϵ) together with pF contours (in black lines). The apparent contrasting behavior of D_p/D_o with respect to density is evident in the two plots; the less-dense soils show the highest D_p/D_o values when the comparison is made with respect to pF (Fig. 7a), whereas the less-dense soils show the lowest D_p/D_o when compared with respect to ϵ (Fig. 7b). Intuitively, compaction decreases diffusivity and hence the denser soils should be expected to exhibit comparatively smaller diffusivity as shown in D_p/D_o vs. pF (Fig. 7a). Note that a soil layer in nature typically stabilizes at a certain matric potential or pF (when sufficient time has elapsed after a rainfall or an irrigation event) rather than at a given air-filled porosity (ϵ), therefore

Fig. 7a exhibits the more realistic representation of diffusivity across density under field conditions. The D_p/D_o vs. ϵ plot, on the other hand, shows the variation between the two directly-related parameters and gives a different perspective from the view of variable soil density (Fig. 7b). Note also that ϵ contours (Fig. 7a) tend to follow the density contours (i.e., color contours) in the upper end (dry region) whereas the pF contours (Fig. 7b) tend to follow the density contours at the lower end (wet region), implying the regions of relative importance for the two parameters with regard to density. Overall, the figure reaffirms that the density-induced effects on gas diffusivity are pronounced at the mid-range in pF (1.75 to 3.75) where sharp changes of ϵ contours and pF contours in both plots were observed.

Despite the data being generated from only a single soil texture the results of this study clearly demonstrate density-induced effects on soil moisture and gas diffusivity control greenhouse gas fluxes. Hence their interaction needs to be considered in grazed pasture systems management. Farmers need to consider using management practices that reduce soil compaction while also optimizing irrigation practices that maximize D_p/D_o . Further research is required to consider the effects observed in the current study with respect to other soil textures, intact soils, and models for predicting D_p/D_o in situ. When the soils are largely structured, bimodal SWC (e.g., Durner, 1994) and D_p/D_o (e.g., Resurreccion et al., 2010) functions need to be considered in place of unimodal func-

Table 1. Basic soil physical characteristics and numerical parameterization.

Physical		Numerical												
Bulk density Mg m^{-3}	Total porosity $\text{m}^3 \text{ m}^{-3}$	Soil-water characteristic Eq. [1]				Soil-gas diffusivity, D_p/D_o Eq. [5]			Cumulative N ₂ O fluxes (% applied) Eq. [6]			Cumulative N ₂ fluxes (% applied) Eq. [7]–[8]		
		θ_r	α	n	m	A	B	C	J_0	J_m	$(D_p/D_o)^*$	J_0	J_m	$(D_p/D_o)^*$
1.1	0.58	0	0.070	3.0	0.15	0.4	5.2	0.04	4.74	0.65	0.038	7.72	0.68	0.038
1.2	0.55	0	0.050	2.5	0.16	0.4	5.2	0.04	4.74	0.65	0.038	7.72	0.68	0.038
1.3	0.51	0	0.038	1.9	0.21	0.4	5.2	0.04	4.74	0.65	0.038	7.72	0.68	0.038
1.4	0.47	0	0.012	1.65	0.30	0.4	5.2	0.04	4.74	0.65	0.038	7.72	0.68	0.038
1.5	0.43	0	0.005	0.94	0.48	0.4	5.2	0.04	4.74	0.65	0.038	7.72	0.68	0.038

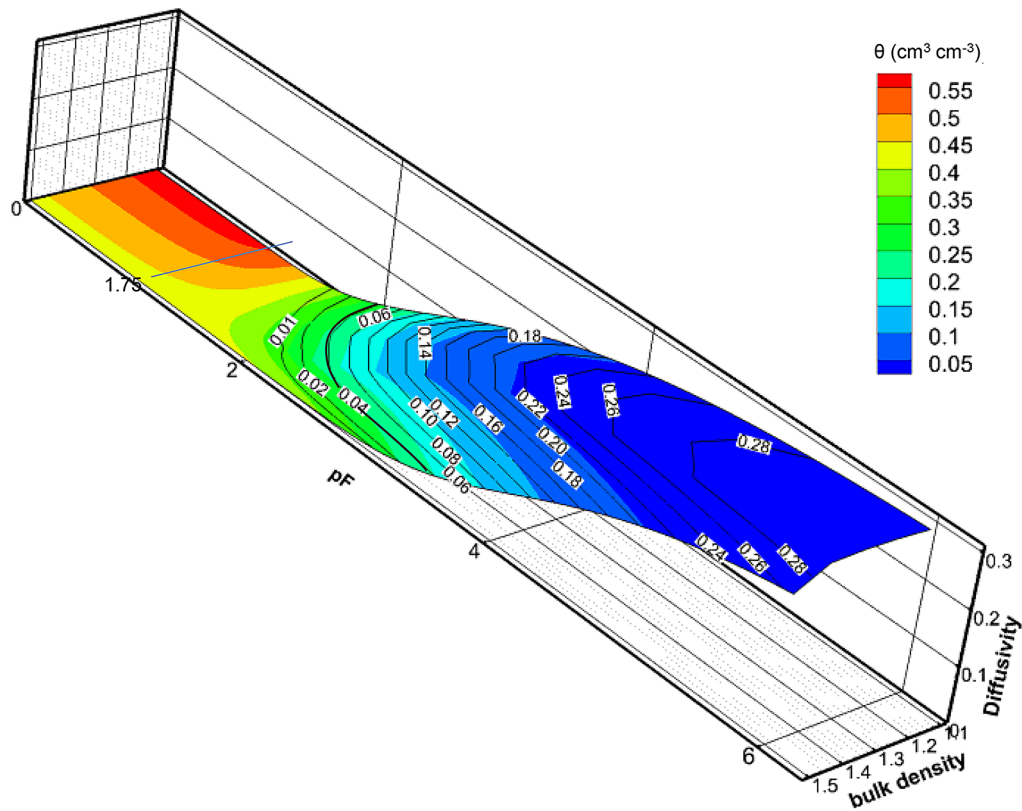


Fig. 6. Three-dimensional representation of the relationship between density, $pF (= \log |\psi, 10^{-1} \text{ kPa}|)$, and gas diffusivity (D_p/D_0). The contour map shows the moisture content ($\theta, \text{cm}^3 \text{cm}^{-3}$) distribution. The black lines show the D_p/D_0 contours. The D_p/D_0 contour corresponding to the threshold diffusivity with respect to N_2O or N_2 emissions, $(D_p/D_0)^*$ (Eq. [6]–[8]), is shown in bold color.

tions. Care should be taken when comparing the results from this controlled laboratory study with those of other studies where different environmental complexities occur, for example the wind- or pressure-induced effects on gas fluxes (e.g., Poulsen and Moldrup, 2006) or temperature-induced changes in gas fluxes (e.g., Elberling et al., 2010) may also play important roles.

CONCLUSIONS

Based on widely-used and proposed parametric functions and using density-related model parameters, this study characterized the density-dependant behavior of soil-water retention, soil-gas diffusivity and cumulative (35-d) N_2O -N and N_2 -N emission fluxes measured in repacked soil sampled from a New Zealand grazed pasture. The measured soil-water characteristic adequately parameterized the van Genuchten (1980) model with model parameters strongly related to density, and further provided useful implications on model-derived density-controlled pore size distributions. We modified a density-corrected soil gas diffusivity model developed originally for intact soils and applied it successfully to repacked soils. Two new proposed functions adequately described the gas-diffusivity-dependent cumulative N_2O -N and N_2 -N

emissions arising from a simulated ruminant urine deposition event. For the soil studied here, the results revealed that the density effects on gas diffusivity and emission fluxes were generally most pronounced in the region of pF of 1.75 to 3.75 where the combined effects of density-dependent moisture retention and gas diffusion were evident. The results suggest that gas diffusivity needs to be maintained above a threshold gas diffusivity, $(D_p/D_0)^*$ ($= 0.038$) irrespective of soil density to minimize the exponential emissions of cumulative N_2O fluxes. We recommend comparing the results of this study with those from other studies with caution as the other environmental complexities unac-

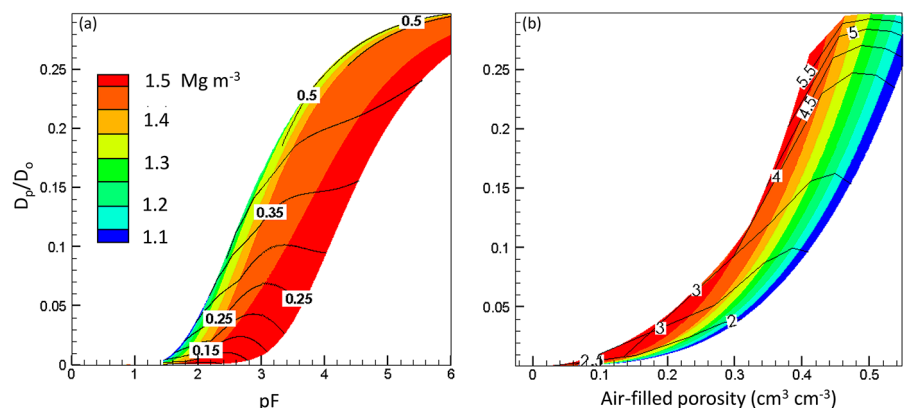


Fig. 7. Variation of soil gas diffusivity (D_p/D_0) against (a) $pF (= \log |\psi, 10^{-1} \text{ kPa}|)$ and (b) air-filled porosity ($\epsilon, \text{cm}^3 \text{cm}^{-3}$) with varying density as shown by the color maps. Solid lines denote ϵ (a) and pF (b) contours, respectively.

counted for in this study (e.g., wind- or temperature-induced effects) may potentially lead to significant disparities in results.

ACKNOWLEDGMENTS

We gratefully acknowledge the financial support for this research from the New Zealand Government and New Zealand Agricultural Greenhouse Gas Research Centre (NZAGRC) under the Livestock Emissions and Abatement Research Network (LEARN) postdoctoral fellowship (LEARN-TECH-AGR-CD-V01). Financial assistance provided by the National Research Council in Sri Lanka (NRC-17-019) is also acknowledged. Any opinion, findings, and conclusions or recommendations expressed herein are those of the authors and do not necessarily reflect the views of those providing technical input or financial support.

REFERENCES

- Allaire, A.E., J. Caron, L.E. Parent, I. Duchesne, and J.A. Rioux. 1996. Air-filled porosity, gas relative diffusivity, and tortuosity: Indices of *Prunus × cistena* sp. growth in peat substrates. *J. Am. Soc. Hortic. Sci.* 121:236–242.
- Balaine, N., T.J. Clough, M.H. Beare, S.M. Thomas, and E.D. Meenken. 2016. Soil gas diffusivity controls N₂O and N₂ emissions and their ratio. *Soil Sci. Soc. Am. J.* 80:529–540. doi:10.2136/sssaj2015.09.0350
- Balaine, N., T.J. Clough, M.H. Beare, S.M. Thomas, E.D. Meenken, and J.G. Ross. 2013. Changes in relative gas diffusivity explain soil nitrous oxide flux dynamics. *Soil Sci. Soc. Am. J.* 77:1496–1505. doi:10.2136/sssaj2013.04.0141
- Ball, B. 2013. Soil structure and greenhouse gas emissions: A synthesis of 20 years of experimentation. *Eur. J. Soil Sci.* 64:357–373. doi:10.1111/ejss.12013
- Breland, T.A., and S. Hansen. 1996. Nitrogen mineralization and microbial biomass as affected by soil compaction. *Soil Biol. Biochem.* 28:655–663. doi:10.1016/0038-0717(95)00154-9
- Buckingham, E. 1904. Contributions to our knowledge of the aeration of soils. *Bur. Soil Bull.* 25. US Gov. Print. Office, Washington, DC.
- Cannell, R.Q. 1977. Soil aeration and compaction in relation to root growth and soil management. *Appl. Biol.* 2:1–86.
- Carter, M.R. 1988. Temporal variability of soil macroporosity in a fine sandy loam under mouldboard ploughing and direct drilling. *Soil Tillage Res.* 12:37–51. doi:10.1016/0167-1987(88)90054-2
- Chamindu Deepagoda, T.K.K., P. Moldrup, P. Schjønning, L.W. de Jonge, K. Kawamoto, and T. Komatsu. 2010. Density-corrected models for gas diffusivity and air permeability in unsaturated soil. *Vadose Zone J.* doi:10.2136/vzj2009.0137
- Clough, T.J., F.M. Kelliher, Y.P. Wang, and R.R. Sherlock. 2006. Diffusion of ¹⁵N-labelled N₂O into soil columns: A promising method to examine the fate of N₂O in subsoils. *Soil Biol. Biochem.* 38:1462–1468. doi:10.1016/j.soilbio.2005.11.002
- Crony, D., and J.D. Coleman. 1954. Soil structure in relation to soil suction (pF). *J. Soil Sci.* 5:75–84. doi:10.1111/j.1365-2389.1954.tb02177.x
- Dick, R.P., D.D. Myrold, and E.A. Kerle. 1988. Microbial biomass and soil enzyme activities in compacted and rehabilitated skid trail soils. *Soil Sci. Soc. Am. J.* 52:512–551. doi:10.2136/sssaj1988.03615995005200020038x
- Drewry, J.J. 2006. Natural recovery of soil physical properties from treading damage of pastoral soils in New Zealand and Australia: A review. *Agric. Ecosyst. Environ.* 114:159–169. doi:10.1016/j.agee.2005.11.028
- Durner, W. 1994. Hydraulic conductivity estimation for soils with heterogeneous pore structure. *Water Resour. Res.* 30:211–223. doi:10.1029/93WR02676
- Elberling, B., H.H. Christiansen, and B.U. Hansen. 2010. High nitrous oxide production from thawing permafrost. *Nat. Geosci.* 3:332–335. doi:10.1038/ngeo803
- Firestone, M.K. 1982. Biological Denitrification. In: F.J. Stevenson, editor, *Nitrogen agricultural soils*. Agron. Monogr. 22. ASA, SSSAJ, and CSA, Madison, WI. p. 289–326.
- Gent, J.A., R. Ballard, and A.E. Hassan. 1983. The impact of harvesting and site preparation on the physical properties of lower coastal plain forest soils. *Soil Sci. Soc. Am. J.* 47:595–598. doi:10.2136/sssaj1983.03615995004700030041x
- Gislerød, H.R. 1982. Physical conditions of propagation media and their influence on the rooting of cuttings. 1. Air content and oxygen diffusion at different moisture tensions. *Plant Soil* 69:445–456. doi:10.1007/BF02372465
- Gupta, S.C., P.P. Sharma, and S.A. Defranchi. 1989. Compaction effects on soil structure. *Adv. Agron.* 42:311–338. doi:10.1016/S0065-2113(08)60528-3
- Hewitt, A.E. 1998. *New Zealand soil classification*, 2nd ed. Manaaki Whenua–Landcare Research New Zealand Ltd., Lincoln, New Zealand.
- Hill, J.N.S., and M.E. Sumner. 1967. Effect of bulk density on moisture characteristics of soils. *Soil Sci.* 103:234–238. doi:10.1097/00010694-196704000-00002
- Hutchinson, G.L., and A.R. Mosier. 1981. Improved soil cover method for field measurement of nitrous oxide fluxes. *Soil Sci. Soc. Am. J.* 45:311–316. doi:10.2136/sssaj1981.03615995004500020017x
- Intergovernmental Panel on Climate Change (IPCC). 2014. *Climate change 2013: The physical science basis*. In: T.F. Stocker, D. Qin, G.-K. Plattner, M. Tignor, S.K. Allen, J. Boschung, A. Nauels, Y. Xia, V. Bex, and P.M. Midgley, editors, *Contribution of Working Group I to the Fifth Assessment Report*. Cambridge Univ. Press, Cambridge, United Kingdom and New York, NY.
- Marshall, T.J. 1959. The diffusion of gases through porous media. *J. Soil Sci.* 10:79–82. doi:10.1111/j.1365-2389.1959.tb00667.x
- Millington, R.J. 1959. Gas diffusion in porous media. *Science* 130:100–102. doi:10.1126/science.130.3367.100-a
- Moldrup, P., T. Olesen, J. Gamst, P. Schjønning, T. Yamaguchi, and D.E. Rolston. 2000. Predicting the gas diffusion coefficient in repacked soil: Water induced linear reduction model. *Soil Sci. Soc. Am. J.* 64:1588–1594. doi:10.2136/sssaj2000.6451588x
- Oenema, O., N. Wrage, G.L. Velhof, J.W. van Groenigen, J. Dolfing, and P.J. Kuikman. 2005. Trends in global nitrous oxide emissions from animal production systems. *Nutr. Cycling Agroecosyst.* 72:51–65. doi:10.1007/s10705-004-7354-2
- Owens, J., T. Clough, J. Laubach, J. Hunt, R. Venterea, and R. Phillips. 2016. Nitrous oxide fluxes, soil oxygen, and denitrification potential from urine and non-urine treated soil under different irrigation frequencies. *J. Environ. Qual.* 45:1169–1177. doi:10.2134/jeq2015.10.0516
- Penman, H.L. 1940. Gas and vapor movements in soil: The diffusion of vapors through porous solids. *J. Agric. Sci.* 30:437–462. doi:10.1017/S0021859600048164
- Ponder, F., and M. Tadros. 2002. Phospholipid fatty acids in forest soil four years after organic matter removal and soil compaction. *Appl. Soil Ecol.* 19:173–182. doi:10.1016/S0929-1393(01)00182-2
- Poulsen, T.G., and P. Moldrup. 2006. Evaluating effects of wind-induced pressure fluctuations on soil–atmosphere gas exchange at a landfill using stochastic modelling. *Waste Manage. Res.* 24:473–481. doi:10.1177/0734242X06066363
- Resurreccion, A.C., P. Moldrup, K. Kawamoto, S. Hamamoto, D.E. Rolston, and T. Komatsu. 2010. Hierarchical, bimodal model for gas diffusivity in aggregated, unsaturated soils. *Soil Sci. Soc. Am. J.* 74:481–491. doi:10.2136/sssaj2009.0055
- Schofield, R.K. 1935. The pF of the water in soil. In: *Trans. World Congr. Soil Sci.*, 3rd, July–Aug. 1935. Vol. 2. Oxford, UK. p. 37–48.
- Selbie, D.R., L.E. Buckthought, and M.A. Shepherd. 2015. The challenge of the urine patch for managing nitrogen in grazed pasture systems. *Adv. Agron.* 129:229–292. doi:10.1016/bs.agron.2014.09.004
- Sigua, G., and S. Coleman. 2009. Long-term effect of cow congregation zone on soil penetrometer resistance, implications for soils and forage quality. *Agron. Sustain. Dev.* 29:517–523. doi:10.1051/agro/2009021
- Taylor, S.A. 1949. Oxygen diffusion in porous media as a measure of soil aeration. *Soil Sci. Soc. Am. Proc.* 14:55–56. doi:10.2136/sssaj1950.036159950014000C0013x
- van Genuchten, M.T. 1980. A closed-form equation for predicting the hydraulic conductivity of unsaturated soils. *Soil Sci. Soc. Am. J.* 44:892–898. doi:10.2136/sssaj1980.03615995004400050002x
- Wrage, N., G.L. Velhof, V.M.L. Beusichem, and O. Oenema. 2001. Role of nitrifier denitrification in the production of nitrous oxide. *Soil Biol. Biochem.* 33:1723–1732. doi:10.1016/S0038-0717(01)00096-7
- Wrage, N., M.A. Horn, R. Well, C. Müller, G. Velhof, and O. Oenema. 2018. The role of nitrifier denitrification in the production of nitrous oxide revisited. *Soil Biol. Biochem.* doi:10.1016/j.soilbio.2018.03.020
- Yahya, Z., A. Husin, J. Talib, J. Othman, S.Z. Darus, O.H. Ahamed, and M.B. Jalloh. 2011. Pores Reconfiguration in Compacted Bernam Series Soil. *Am. J. Appl. Sci.* 8:212–216. doi:10.3844/ajassp.2011.212.216